Journal of Power Sources 189 (2009) 522–526

Contents lists available at ScienceDirect

Journal of Power Sources

journal homepage: www.elsevier.com/locate/jpowsour

Short communication

$LiFePO_4$ as an optimum power cell material

L.Q. Sun[a], R.H. Cui[a], A.F. Jalbout[b], M.J. Li[a], X.M. Pan[a], R.S. Wang[a,*], H.M. Xie[a,*]

[a] Institute of Functional Materials, Faculty of Chemistry, Northeast Normal University, Changchun, Jilin 130024, PR China
[b] NASA Astrobiology Institute and the Department of Chemistry, The University of Arizona, Tucson, AZ 85721, USA

ARTICLE INFO

Article history:
Received 13 August 2008
Received in revised form 20 October 2008
Accepted 29 October 2008
Available online 8 November 2008

Keywords:
$LiFePO_4$
Polyacence
Lithium ion batteries
Power cells

ABSTRACT

Nano-crystallized $LiFePO_4$ has been synthesized with a simple three-step-synthesis technology in the presence of nano-ferric oxide as iron source and polyacence (PAS) as a reductive agent and high conductive carbon source. The use of PAS increases the conductivity and prevents the particles growth. The most feasible calcined temperature and time was investigated and the best cell performance was delivered by the sample calcined at 700 °C for 4 h. This material shows excellent specific capacity and cycle efficiency at high current rates, almost no capacity loss can be observed up to 100 cycles which make it more superior as an optimum power cell cathode material.

1. Introduction

Lithium iron phosphate is novel and an important member of cathode material for lithium ion batteries. Numerous research efforts laid the steady foundation of the development of $LiFePO_4$ [1–9]. Several modifications and treatments of $LiFePO_4$ have been used to improve the electrochemical performance for its large-scale manufacture. Carbon coating [10–17] is an alternative method on enhancing the specific capacity and rate capability.

Various carbon atoms have been implemented in previous researches. The conductive carbon coating on particle surfaces can improve the electronic conductivity of $LiFePO_4$ and act as dispersion among the particles to prevent the particles growth [18,19].

We have used a self-made $FePO_4{\cdot}2H_2O$ as precursor and designed a core/shell compound that consists of the spherical $LiFePO_4$ structure coated by the specific π-bond character planar polymer (polyacence, PAS). The electronic conductivity, low-temperature character, and the tap density of a $LiFePO_4$–PAS composite were all rapidly improved simultaneously [20]. Nevertheless, the limitation of our previous procedure is the long reaction time for the preparation of $FePO_4{\cdot}2H_2O$, which hindrances the application of this method for the industrial concern.

The simplification of technology and the tap density are all actually connected with the choices of the raw materials. We use nano-ferric oxide as the source of iron combined with the carbon source of PAS to construct an optimum simply synthetic technology more fitted the industrialization which only include grinding, spray-drying and calcining. The sample tap density is much higher than that synthesized by gas production method. Special quenching technology was employed and the most optimal calcined temperature and time was provided.

2. Experimental

$LiFePO_4$–PAS was synthesized using lithium dihydrogen phosphate (LiH_2PO_4) and ferric oxide (Fe_2O_3) in a stoichiometric molar ratio (1:0.5). The precursors were mixed with an 8 wt% of phenol–formaldehyde resin dissolved in a small quantity of ethanol, and its pyrolyzate is polyacence (PAS). The mixture was ball-milled in water for 5 h and then spray-dried at 180 °C with air as the carrier gas, and calcined under N_2 gas for 2, 4, 6 and 8 h at the heating rate of 3 °C min^{-1} at various temperature 600, 700, 750 and 800 °C, respectively.

Structural analysis and phase purity were analyzed by a powder X-ray diffractometer (XRD), Siemens D-5000, Mac Science MXP18, equipped with a nickel-filtered Cu Kα radiation source (λ = 1.5406 Å). The surface morphology of the powders was observed with a field emission scanning electron microscope (FE-SEM) and transmission electron microscope (TEM). Coin cells of the 2025 configuration were assembled in an argon-filled glove box

* Corresponding authors. Tel.: +86 431 85099511; fax: +86 431 85099511.
E-mail addresses: wangrs@nenu.edu.cn (R.S. Wang), xiehm136@nenu.edu.cn (H.M. Xie).

0378-7753/$ – see front matter © 2008 Elsevier B.V. All rights reserved.
doi:10.1016/j.jpowsour.2008.10.120

in which the oxygen and water contents were maintained below 2 ppm. The cells are assembled as follows: cathode shell | cathode active materials ($LiFePO_4$:PTFE:carbon black = 84:8:8) | electrolyte ($LiPF_6$/EC:DEC = 1:1) | membrane | electrolyte ($LiPF_6$/EC:DEC = 1:1) | anode (lithium sheet) | nickel-net current collector | anode shell. The cells were tested in the equipment Land Battery Test System.

3. Results and discussion

3.1. Tap density

Comparison among different $LiFePO_4$ synthesis routes, the tap density is varied. We have selected ferric oxide and lithium dihydrogen phosphate as a precursor source. There is almost no emission except for a little carbon dioxide generated from the pyrolysis of PAS. What were obtained was a solid sphere particles and the tap density is improved to 1.5 g cm^{-3}. The tap density of gas production method ($FeC_2O_4{\cdot}2H_2O$, $NH_4H_2PO_4$ and Li_2CO_3 as raw materials) is about 1.0 g cm^{-3}, and it is perhaps due to so many gases generated, which disperse the particles further and make the samples much looser.

3.2. X-ray diffraction

X-ray diffraction patterns of $LiFePO_4$–PAS powders heat treated for 4 h at different temperatures from 600 to 800 °C are shown in Fig. 1. The lattice constants were as follows: $a = 10.368$; $b = 5.99$; $c = 4.695$ (600 °C); $a = 10.303$; $b = 5.951$; $c = 4.693$ (700 °C); $a = 10.309$; $b = 5.983$; $c = 4.69$ (750 °C); $a = 10.35$; $b = 5.993$; $c = 4.6925$ (800 °C). All samples reveal a single-phase $LiFePO_4$ with an ordered olivine structure indexed by orthorhombic *Pnma* (JCPDS card no. 83-2092). The value b is the smallest at 700 °C which is helpful to Li^+ diffusion. Lack of impure phases was observed in the as-prepared $LiFePO_4$. Here, we can see that there is a little broad region from 20 to 30° for the samples synthesized at 600 °C and the broad region disappeared when the temperature is higher than 750 °C, which suggests that the carbon generated from phenol–formaldehyde resin is transformed from amorphous carbon to ordered polyacence (PAS). Furthermore, it is found that the peaks gradually sharpen with increasing temperature. The relative intensity of the X-ray diffraction patterns of the $LiFePO_4$ powders becomes the strongest when the temperature is up to 800 °C, which

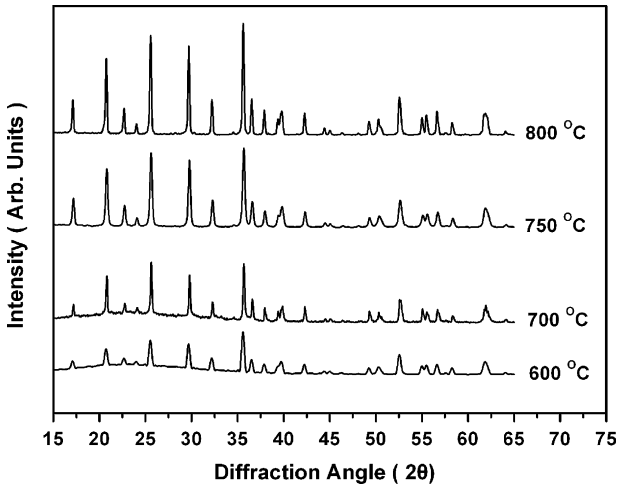

Fig. 1. XRD patterns of $LiFePO_4$–PAS powders prepared at different temperatures.

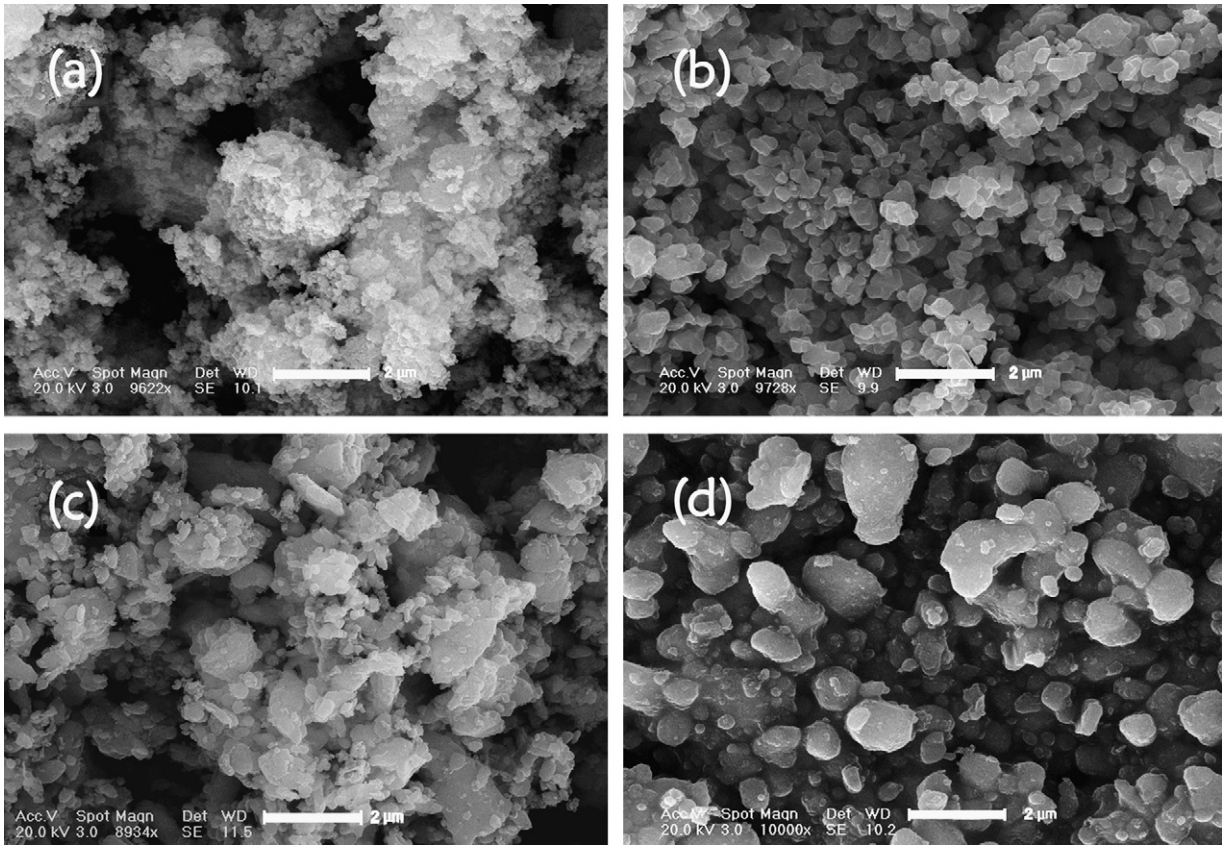

Fig. 2. SEM morphology of $LiFePO_4$–PAS powders prepared at different temperatures: (a) 600 °C, (b) 700 °C, (c) 750 °C and (d) 800 °C.

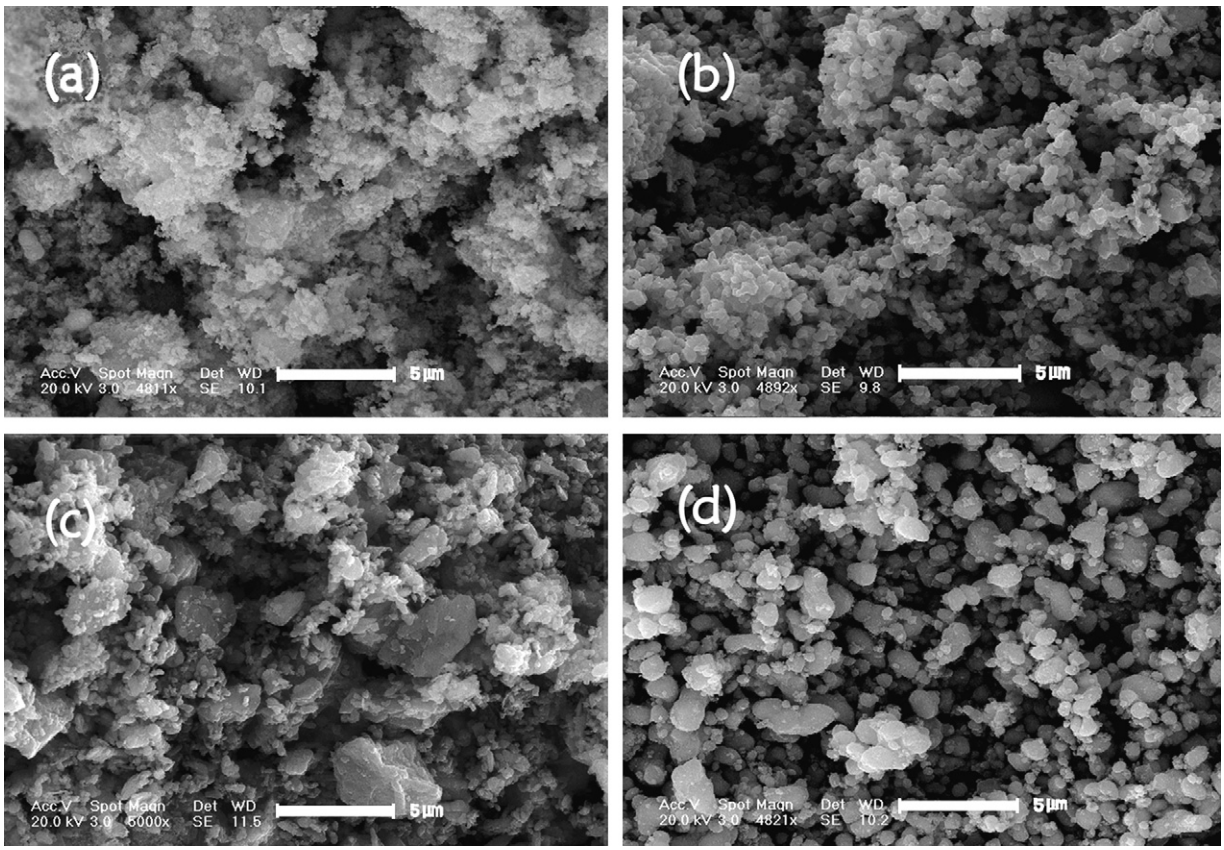

Fig. 3. SEM morphology of $LiFePO_4$–PAS at 700 °C with different sintering time: (a) 2 h, (b) 4 h, (c) 6 h and (d) 8 h.

indicates an increase of crystallinity as occur from growth of grain size, ordering of local structure, and release of lattice strain [21,17].

3.3. Effect on the sample morphology at different calcined temperatures

The morphology for the $LiFePO_4$–PAS powders, which have been synthesized for 4 h at 600, 700, 750 and 800 °C and then quenched to room temperature, was observed on SEM (Fig. 2). Fig. 2a shows some irregular powders at 600 °C due to the amorphous particles, and this is also confirmed by XRD result where broad region appear at 600 °C (see Fig. 1). The degree of crystallization was intact at 700 °C, with a lot of independent nano-sized particles obtained. With the temperature rising to 750 °C, and eventually to 800 °C, the particles begin growing from 500 nm to 1 μm.

The crystallinity is much higher while it shows the agglomeration among particles when the temperature is over 750 °C. It is in good agreement with the XRD observations, in which the amorphous formed carbon is transformed into more orderly PAS and the sample crystallinity and the particles size all increase with the increase of heat-treatment temperature. As it is known, the particle size is a crucial factor to the lithium ion diffusion in $LiFePO_4$ [22]. Thus the most feasible sintering temperature that we choose is 700 °C.

3.4. Effect on the sample morphology at different calcined time

To explore the most optimum sintering time, the precursor was calcined at 700 °C for 2, 4, 6 and 8 h, respectively, and then quenched to room temperature. In Fig. 3, we can see that the sample calcined for 4 h gives fine crystal in the range of 200–300 nm with a narrow particle size distribution. When the preparing time was enhanced to 6 h, the crystal grains grow and accompany with the agglomeration. With the sintering time further increasing to 8 h, the sizes of the particles become even bigger. Therefore, the sintering time must be controlled. Shortening the sintering time is contributed to preventing the particles' growth. The optimum heat-treatment temperature and time have controlled the crystal grain growth, further shortened the diffusion length and improved the lithium ion mobility [17,23].

3.5. Transmission electron microscope and Infrared spectra

Infrared spectra (IR) and transmission electron microscopy (TEM) have been used to make an investigation of the carbon coated layer of $LiFePO_4$. Herein, PAS, as a high conductive carbon, was used to synthesize coated $LiFePO_4$ compounds. The TEM image shows that $LiFePO_4$ powders (synthesized at 700 °C for 4 h) are covered with a carbon layer (Fig. 4). The dark region is $LiFePO_4$ and the light grey region is carbon, indicating that the $LiFePO_4$ is surrounded by carbon. To further confirm the coating of PAS, we ran this sample infrared spectrum analysis, as shown in Fig. 5. The absorptions at about 748, 1480 and 1610 cm^{-1} of the IR spectrum are in reference to =CH out-of-plane deformation vibration of substituted benzene and the stretching vibration of the aromatic ring C=C. The others are assigned to characteristic peaks of $LiFePO_4$. Therefore, the PAS is formed completely at 700 °C.

3.6. Electrochemical properties

The electrochemical performance of the synthesized $LiFePO_4$ depended strongly on the sintering temperature and time, as shown

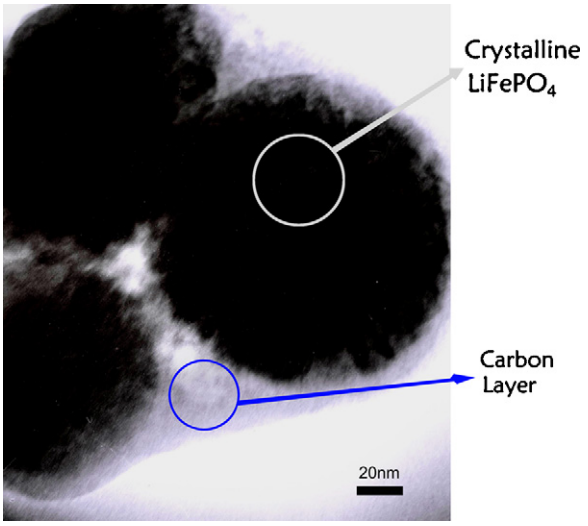

Fig. 4. TEM image of $LiFePO_4$-PAS prepared at 700 °C for 4 h. Carbon is depicted as grey and $LiFePO_4$ as black.

in Fig. 6. On the basis of the discharge capacity, the best result is the sample calcined at 700 °C for 4 h, which first-cycle discharge capacity was 159.7 mAh g^{-1} at the 0.2 C rate. The initial discharge capacity of $LiFePO_4$–PAS increased first and decreased afterwards with the increasing temperature (Fig. 6a) and time (Fig. 6b). The reason can be attributed to the optimal particle size and the crystallinity is 700 °C for 4 h, which was confirmed by the XRD and SEM patterns.

The sample of the $LiFePO_4$–PAS in our experiments exhibits relatively excellent rate capability and cycling performance at various charge–discharge rates (Fig. 7). The specific capacity is about 141.3 mAh g^{-1} at 1 C rate, and 120 mAh g^{-1} at 5 C, even 104 mAh g^{-1} at 10 C, and the retention is 99% after 100 cycles. In this experiment, the cells were charged to 4.2 V and discharged to 2.5 V at given rates.

The cycling performance of $LiFePO_4$–PAS commercial cells that use graphite and $Li_4Ti_5O_{12}$ separate anodes has been addressed in Fig. 8. It was charged and discharged at 1 C rate, and the cell capacity shows no attenuation after 1000 charge–discharge cycles.

High conductive PAS covers the $LiFePO_4$ particles surface that improves the electron conductivity to 10^0–10^1 S cm^{-1}. The high rate capability and excellent cycle performance should be attributed to the enhanced electronic conductivity of the material resulting from PAS coating and the improved ion mobility resulting from controlling the particle size and degree of crystallization.

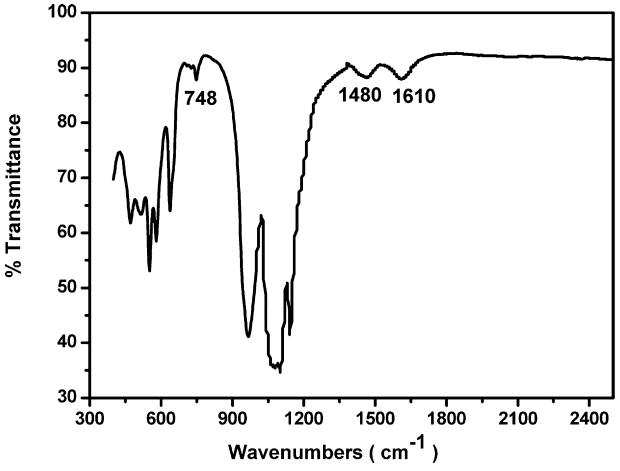

Fig. 5. IR absorption spectra of $LiFePO_4$–PAS at 700 °C.

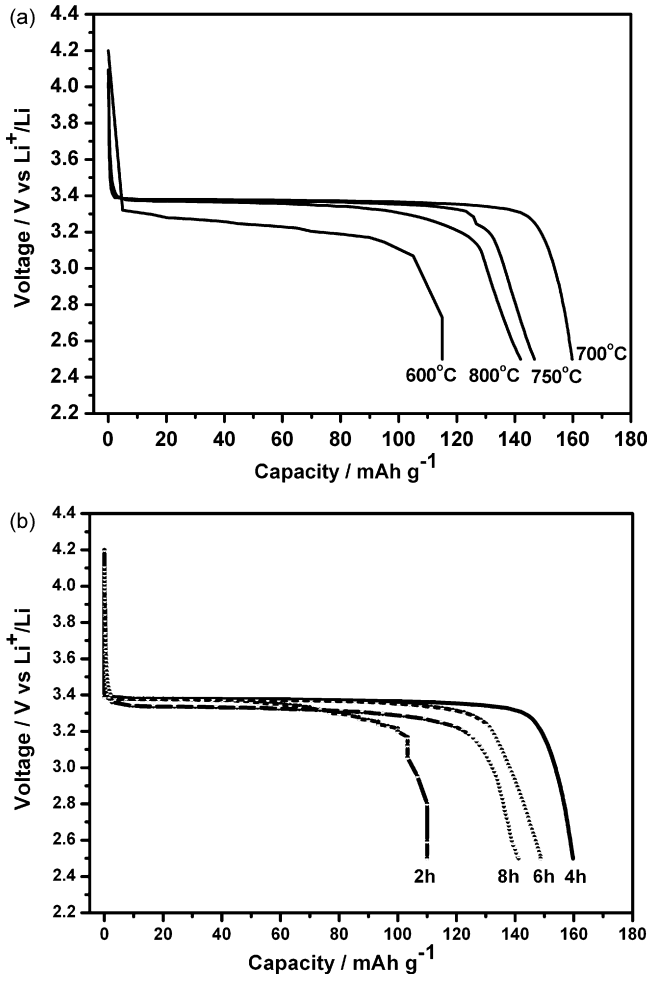

Fig. 6. (a) The initial discharge curves of $LiFePO_4$–PAS composites obtained at different temperatures which were calcined for 4 h and (b) the initial discharge curves of $LiFePO_4$–PAS composites obtained at 700 °C calcined for 2, 4, 6 and 8 h.

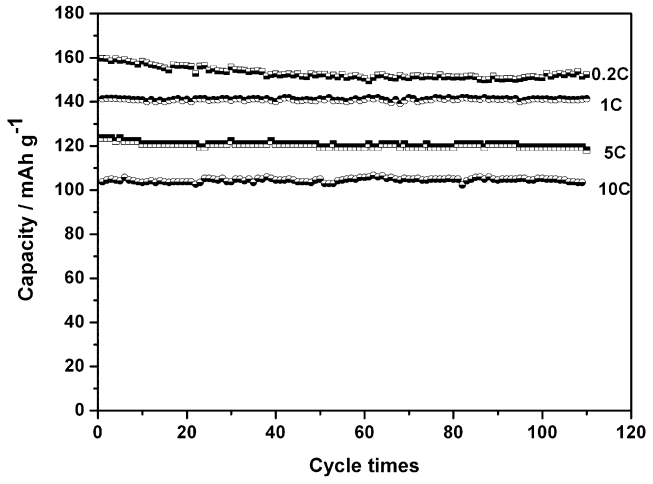

Fig. 7. The cycle performance of the $LiFePO_4$–PAS prepared at 700 °C calcined for 4 h at different rates.

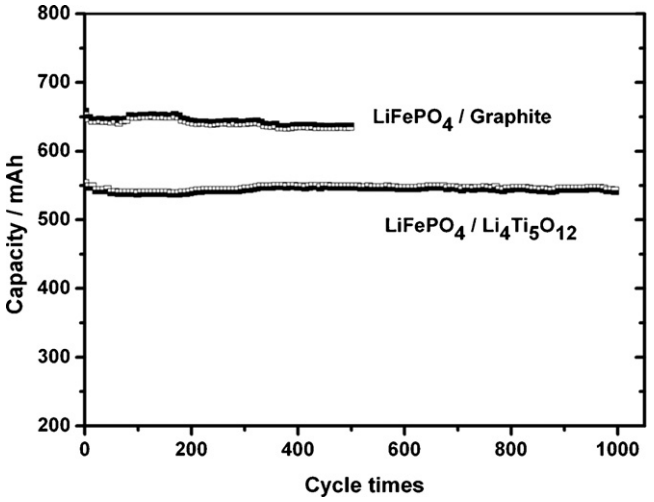

Fig. 8. The cycle performance of the $LiFePO_4$–PAS commercial cell.

4. Conclusions

Simple synthesis technology adequate for industrialization was provided by analyzing the influence of different heat-treatment temperature and time. The product which was prepared at 700 °C for 4 h yields smaller, more uniform particles and better electrochemical performance. A high conductive polymer–polyacence (PAS) has been implemented as an effective carbon source to synthesize smaller and homogeneous $LiFePO_4$–PAS cathode materials. $LiFePO_4$–PAS has become the most optimum power cell cathode material due to its high relative tap density, high rate performance and long cycle life.

Acknowledgements

This work was supported by a project issued by the Science and Technology Development Program of the Jilin Province (grant No. 20076020, No. 20080304), and Training Fund of NENU'S Scientific Innovation Project (07016).

References

[1] A.K. Padhi, K.S. Nanjundaswamy, J.B. Goodenough, J. Electrochem. Soc. 144 (1997) 1188.
[2] S.-Y. Chung, J.T. Bloking, Y.-M. Chiang, Nat. Mater. 1 (2002) 123–128.
[3] S. Franger, F. Le Cras, C. Bourbon, H. Rouault, J. Power Sources 119–121 (2003) 252–257.
[4] S. Okada, T. Yamamoto, Y. Okazaki, J.-I. Yamaki, M. Tokunaga, T. Nishida, J. Power Sources 146 (2005) 570–574.
[5] P. Subramanya Herle, B. Ellis, N. Coombs, L.F. Nazar, Nat. Mater. 3 (2004) 147–152.
[6] C. Delacourt, P. Poizot, J.-M. Tarascon, C. Masquelier, Nat. Mater. 4 (2005) 254–260.
[7] A. Yamada, H. Koizumi, S.-I. Nishimura, N. Sonoyama, R. Kanno, M. Yonemura, T. Nakamura, Y. Kobayashi, Nat. Mater. 5 (2006) 357–360.
[8] Y. Watanabe, H. Morimoto, S. Tobishima, J. Power Sources 154 (2006) 246–254.
[9] Y.Q. Wang, J.L. Wang, J. Yang, Y. Nuli, Adv. Funct. Mater. 16 (2006) 2135–2140.
[10] Z.H. Chen, J.R. Dahn, J. Electrochem. Soc. 149 (2002) A1184–A1189.
[11] J.-K. Kim, J.-W. Choi, G. Cheruvally, J.-U. Kim, J.-H. Ahn, G.-B. Cho, K.-W. Kim, H.-J. Ahn, Mater. Lett. 61 (2007) 3822–3825.
[12] G.X. Wang, L. Yang, S.L. Bewlay, Y. Chen, H.K. Liu, J.H. Ahn, J. Power Sources 146 (2005) 521–524.
[13] G.T.-K. Fey, T.-L. Lu, J. Power Sources 178 (2008) 807–814.
[14] J. Moskon, R. Dominko, R. Cerc-Korosec, M. Gaberscek, J. Jamnik, J. Power Sources 174 (2007) 683–688.
[15] M.M. Doeff, J.D. Wilcox, R. Kostecki, G. Lau, J. Power Sources 163 (2006) 180–184.
[16] H.C. Shin, W. Cho II, H. Jang, J. Power Sources 159 (2006) 1383–1388.
[17] L.N. Wang, X.C. Zhan, Z.G. Zhang, K.L. Zhang, J. Alloys Compd. 456 (2008) 461–465.
[18] K.F. Hsu, S.Y. Tsay, B.J. Hwang, J. Mater. Chem. 14 (2008) 2690–2695.
[19] H. Huang, S.-C. Yin, L.F. Nazar, J. Electrochem. Soc. 149 (2002) 1184.
[20] H.M. Xie, R.S. Wang, J.R. Ying, L.Y. Zhang, A.F. Jalbout, H.Y. Yu, G.L. Yang, X.M. Pan, Z.M. Su, Adv. Mater. 18 (2006) 2609–2613.
[21] S.S. Zhang, J.L. Allen, K. Xu, T.R. Jow, J. Power Sources 147 (2005) 236.
[22] A. Yamada, S.C. Chung, K. Hinokuma, J. Electrochem. Soc. 148 (2001) A224.
[23] C. Xu, J. Lee, A.S. Tej, J. Supercrit. Fluids 44 (2008) 92–97.